Trees (2020) 34:89–99
https://doi.org/10.1007/s00468-019-01899-2

ORIGINAL ARTICLE

The adjustment of *Prosopis tamarugo* hydraulic architecture traits has a homeostatic effect over its performance under descent of phreatic level in the Atacama Desert

Marco Garrido[1,2] · Horacio Bown[3] · José Ayamante[2] · Magda Orell[3] · Andrea Sánchez[2] · Edmundo Acevedo[2]

Received: 1 April 2019 / Accepted: 10 August 2019 / Published online: 24 August 2019
© Springer-Verlag GmbH Germany, part of Springer Nature 2019

Abstract

Key message *Prosopis tamarugo* undergoes several modifications of its hydraulic architecture, which has a homeostatic effect on its performance under descent of phreatic level.

Abstract Groundwater extraction for mining has generated a large area of descent of phreatic level in the Llamara Salt Flat, Atacama Desert, where *Prosopis tamarugo* lives as a strict phreatophyte. We study different hydraulic architecture traits of *P. tamarugo* after 12 years of exposure to a descent of phreatic level of ~ 11 m to assess its acclimation capacity. Under this condition, tree size was reduced making the structure of trees shrubbier. At branch level, leaf shedding increased Huber Value and theoretical leaf-specific hydraulic conductivity. At vascular tissue level, vessel composition decreased significantly due to an increase in vessel density and a slight decrease in mean vessel area. This meant that there were no differences of theoretical sapwood-specific hydraulic conductivity and wood density between conditions of descent of phreatic level. Although the theoretical hydraulic efficiency is high under descent of phreatic level, a lower midday water potential indicates other possible factors that may affect its performance (e.g., microclimate, daily loss of conductivity and a high root resistances). The above is consistent with a higher leaf mass per area of the remaining leaves, but no differences were observed in stomatal conductance, leaf ^{13}C isotopic composition and predawn water potential between descent condition. While the adjustment of hydraulic architecture traits has a homeostatic effect on *P. tamarugo* performance, it is necessary to evaluate the limits of its resistance to contribute to its conservation in a context of intervention of its habit, mainly due to demographic growth and non-metallic mining.

Keywords Phreatophyte · Water stress · Wood density · Vascular anatomy · Theoretical sapwood-specific hydraulic conductivity

Communicated by Nardini.

Electronic supplementary material The online version of this article (https://doi.org/10.1007/s00468-019-01899-2) contains supplementary material, which is available to authorized users.

✉ Marco Garrido
marcogarrido@uchile.cl

[1] Centro de Estudios de Zonas Áridas, Facultad de Ciencias Agronómicas, Universidad de Chile, Las Cardas s/n, Coquimbo, Chile

[2] Departamento de Producción Agrícola, Facultad de Ciencias Agronómicas, Universidad de Chile, Casilla 1004, Santiago, Chile

[3] Facultad de Ciencias Forestales y de la Conservación de la Naturaleza, Universidad de Chile, Casilla 1004, Santiago, Chile

Introduction

The Llamara Salt flat (lat − 21.350921° long − 69.657203°) is a basin located in the Pampa del Tamarugal National Reserve, Atacama Desert, northern Chile. In this environment, a thorny forest of very low density is located, where *Prosopis tamarugo* is the most abundant plant species. *P. tamarugo* is a legume tree endemic to the Atacama Desert, adapted to the high thermal oscillation and solar radiation of the desert (Lehner et al. 2001, Chávez et al. 2013). The species is considered a strict phreatophyte that performs hydraulic lifting from the groundwater to the surface soil through pivoting roots, also exhibiting a superficial fasciculate system that develops in a condition of high soil salinity (Sudzuki 1969; Aravena and Acevedo 1985). Given the absence of rainfall in its environment (Hacke et al. 2006),

the Llamara aquifer is the only significant source of water for the species. The extraction of water for use in mining has generated a large area of descent of phreatic level, diminishing the water availability for *P. tamarugo*, a key factor in the performance of the plants and one of the main sources of variation of traits associated with its function and structure (Maherali et al. 2004; Lambers et al. 2008).

In the medium and long term, tree functional homeostasis would be determined by adjustments of its hydraulic architecture (HA), i.e., the hydraulic design that influences the movement of water from roots to leaves, and therefore defines the amount of water, which can be provided to the canopy (Cruiziat et al. 2002; Cosme et al. 2017). Among the components of the HA are listed the maximum hydraulic conductivity, hydraulic vulnerability (P_{50}), tissue capacitance, tree height (H) and Huber Value (HV; sapwood to leaf area ratio) (Sperry et al. 1988; Tyree and Ewers 1991; Cruiziat et al. 2002; Meinzer et al. 2009; Jupa et al. 2016). In addition, other functional traits have been considered by its integrative character, such as leaf mass per area and wood density (Cosme et al. 2017). A high leaf mass per area is associated with low water potential at leaf turgor loss point (Bucci et al. 2004; Johnson et al. 2018) and water potential at 50% loss of leaf hydraulic conductance (Johnson et al. 2018), while wood density is a complex trait that could integrate mechanical and hydraulic properties of tissue, e.g., vessel implosion tolerance and capacitance (Hacke et al. 2001; Bucci et al. 2004; Zanne et al. 2010). Although denser wood can be associated with narrow vessels and a low vessels density that result in a low volume of lumen (Preston et al. 2006), fibers fraction must be considered because its thick cell walls contributing to wood density (Fortunel et al. 2013), and ultimately the variation in tissue composition as being the primary determinant of wood density (Poorter et al. 2010; Zanne et al. 2010; Zanne and Falster 2010).

The inter-specific variability of the HA has been evaluated in several biomes, observing a hydraulic efficiency–safety trade-off, i.e., a trade-off between water transport capacity and tolerance to low water potential (Tyree et al. 1994; Sperry et al. 2008; Maherali et al. 2004). At a xylematic tissue level, this trade-off is shown through an inter-specific positive association between sapwood-specific hydraulic conductivity and P_{50} (Maherali et al. 2004). Therefore, the decrease in water transport efficiency imposed by the environment is compensated by increasing the hydraulic safety of the system (lower P_{50}, Sperry et al. 2008). This is achieved by investing in xylem vessels of smaller diameter (Sperry and Saliendra 1994; Meinzer et al. 2009) associated with higher wood density (Hacke et al. 2001; Bucci et al. 2004; Fortunel et al. 2013). Although HA plasticity constitutes a key acclimation mechanism to drought (Tyree and Ewers 1991), there are few studies that evaluate response patterns of intra-specific hydraulic architecture depending on the availability of water, and even less under the same meteorological conditions (Zolfaghar et al. 2015).

Addington et al. (2006) observed that *Pinus palustris* in a xeric habitat was shorter, had lower HV and a higher root area: foliar area ratio than in a mesic habitat. These adjustments have homeostatic effects that allow *P. palustris* to maintain similar stomatal conductance in different environments. Martínez-Vilalta et al. (2009) observed in *Pinus sylvestris* a negative association between environmental aridity and leaf area:sapwood area ratio, and a positive correlation with leaf-specific hydraulic conductivity although trees exhibited foliage shedding; however, no P_{50} differences were observed in branches. In phreatophytes, Zolfaghar et al. (2015) observed that *Eucalyptus* trees subject to deeper phreatic level have lower P_{50} in branches and higher HV. However, they did not observe differences in branch sapwood-specific hydraulic conductivity or wood density. A similar trend was observed in *Banksia attenuata* and *B. menziesii*, facultative phreatophytes that, growing in upper dunes with greater aridity, developed a vascular tissue more tolerant to embolism than trees established in the more humid lower part (Canham et al. 2009). In *P. tamarugo,* it has been observed that in a condition of descent of phreatic level, there are shorter trees (Garrido et al. 2018), lower radial stem growth (Decuyper et al. 2016), drought induced leaf shedding (Chávez et al. 2013) and increased leaf mass per area (Garrido et al. 2018), which gives evidence of adaptation. However, the degree of adaptation of other HA traits and their influence on the performance of *P. tamarugo* under prolonged descent of phreatic level remain unknown.

In this study, traits associated with the hydraulic architecture of *P. tamarugo* at the vascular tissue, organ and whole tree level were evaluated with the aim to know the species' plasticity after 12 years of exposure to severe descent of water table. Our working hypothesis is that in a condition of descent of phreatic level, *P. tamarugo* adjusts its HA by increasing its hydraulic safety in relation to a control condition, with homeostatic effects on the performance of *P. tamarugo* in the Llamara Salt Flat, Atacama Desert.

Materials and methods

Study site, experimental setup and sampling

The study was carried out during the summer season 2017–2018 in the Llamara Salt Flat located in the Atacama Desert, northern Chile (Fig. 1; lat − 21.350921° long − 69.657203°). In this area, there is an arborescent shrub forest consisting of *P. tamarugo* (< 10% coverage) and *Caesalpinia aphylla* (< 25% coverage). Llamara Salt Flat has a tropical hyper-arid bioclimate (Leubert and Pliscoff

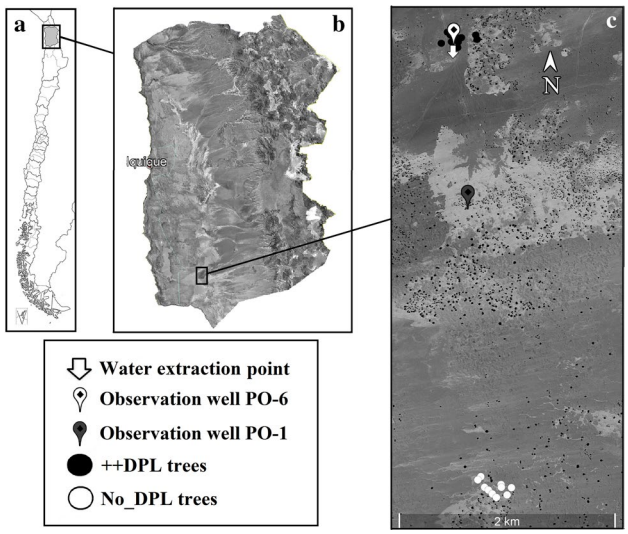

Fig. 1 Location of Llamara Salt Flat (lat − 21.350921° long − 69.657203°), Atacama Desert, northern Chile (**a** and **b**), and position of *Prosopis tamarugo* trees (No_DPL and ++DPL trees), observation wells (PO-6 y PO-1) and groundwater pumping well in the study area (**c**)

2006) characterized by an almost absolute absence of precipitation, a high thermal oscillation, low relative humidity, and high incident radiation. For detailed information about the site, see Chávez et al. (2013) and Calderón et al. (2015).

In Llamara Salt Flat, groundwater has been pumped for use in mining since December 2005, which has generated a descent of phreatic level (DPL) expresses as a depression cone, i.e., DPL increases whit the distance from the groundwater pumping well (Chávez et al. 2013; Garrido et al. 2016, 2018). For this study, we select two groups of ten *P. tamarugo* trees. The first group called ++DPL was closest to the pumping well. The second group called No_DPL was a control group located 4 km in a linear transect (Fig. 1c).

In the study area, there are two observation wells used to monitor the current depth of phreatic level from the beginning of groundwater pumping to the date (Fig. 2). The observation well PO-6 indicates that *P. tamarugo* trees growing in ++DPL have experienced a descent of phreatic level of ~ 11 m from 2005 to the summer season 2017–2018, when this study was conducted. The observation well PO-1 located 1.5 km above the linear transect between groundwater pumping well and No_DPL trees has experienced a descent of phreatic level of only ~ 1.5 m (Fig. 2) from 2005; it is so we consider that *P. tamarugo* trees in No_DPL have grown outside the influence of the groundwater pumping well.

Branch, twigs and leaves sampling, as well as measurements of stomatal conductance, water potential and twig elongation rate were made on the northeastern face of each tree at ~ 1.7-m height, where the environmental conditions were more homogeneous during the day (radiation and wind). We collected third-order branches (diameter from ~ 1 to 2 cm and ~ 60 cm long) for wood density and anatomy, and three terminal twigs per tree from the last growing season were also sampled (ideally belonging to the sampled branches) for twig Huber Value and leaf mass per area measurements. All the samples were placed in plastic bags, which had absorbent paper saturated with water to avoid dehydration and were transported in cold in plastic containers for its processing in the laboratory.

Tree height, wood density and twig elongation

The height (H; m) of each tree was measured in the field with a Tandem-360R/PC clinometer (Suunto, Finland). The largest and smallest diameter of the crown, and the perimeter of

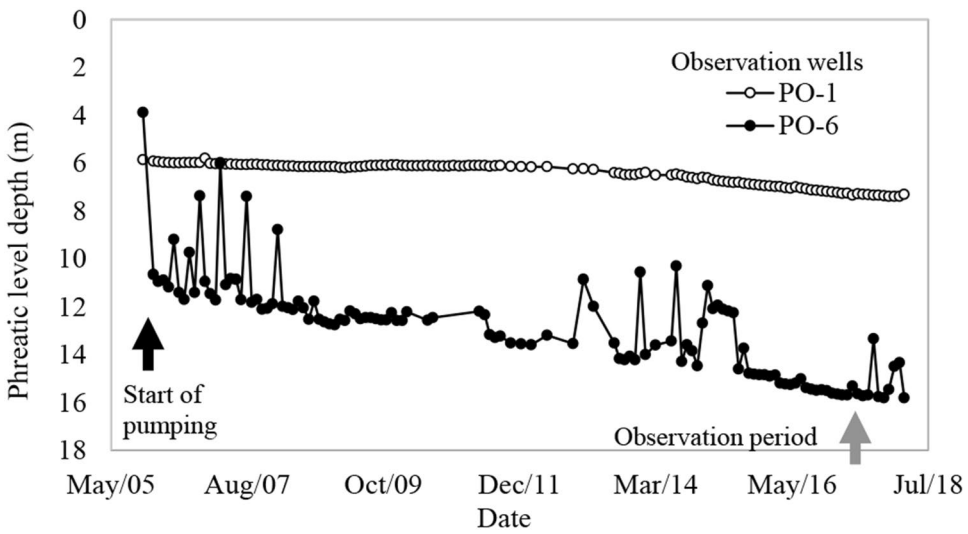

Fig. 2 Depth of the phreatic level of study area in the Llamara Salt Flat, Northern Chile from 2005 to 2018. Observation well PO-6 (~ 11 m of descent of phreatic level from 2005) and PO-1 (~ 1.5 m of descent of phreatic level from 2005) are located at 500 m and 1.5 km from de groundwater extraction well, respectively. The time when groundwater pumping begins, and this study was carried out are indicated by a black and gray arrow, respectively

each trunk were measured with a measuring tape to estimate the crown area (CA; m^2) and total trunk cross-sectional area (sCSA; m^2), respectively.

Wood density (WD; g cm^{-3}) was estimated as the ratio between the dry mass of a wood sample and its fresh volume. The measurement was made in three cylindrical internodes segments, without thorns or twigs, per branch sampled. Each segment was placed in distilled water for 12 h, then the bark was removed, and their volume was determined through a dimensional method (Pérez et al. 2013) measuring the length and diameter of regular branch cylinders (average between the beginning, middle, and end of the segment). Subsequently, the segments were dried in a forced air oven (Venticell, MMM Group, Deutschland) at 70 °C until constant weight, and then their dry mass determined.

In each tree, four buds actively growing were marked and measured when being less than ~ 1 cm in length. After 10 days, the measurement was repeated. Finally, the twig relative elongation rate (RER; mm mm^{-1} day^{-1}) was estimated as follows:

$$\mathrm{RER} = \frac{\mathrm{Length_t} - \mathrm{Length_{ini}}}{\mathrm{tLength_{ini}}}, \quad (1)$$

where $\mathrm{Length_t} - \mathrm{Length_{ini}}$ was the difference in twig length between two consecutive times (10 days), and Length_{ini} is the initial length of the twig.

Water potential and minimum stomatal conductance

Predawn water potential (Ψ_{pd}; MPa) was measured in two twigs per tree between 4:00 and 6:00 h. To define the moment of minimum water potential (Ψ_{md}; MPa) and stomatal conductance (g_s; mol m^{-2} s^{-1}), daily cycles were performed on four trees per DPL condition during two consecutive days (Supplementary Fig. 1). Based on the results, we measure g_s and Ψ_{md} between 13:00 and 15:00 h to represent the minimum daily values.

The Ψ_{md} was measured with a pressure chamber model 1505D EXP (PMS Instrument Company, USA) following a standard methodology (Scholander et al. 1965). Four twigs naturally exposed to solar radiation per tree were covered with aluminum and plastic foil for 2 h prior to the measurement to suppress twig transpiration with the aim of equilibrating the water potential of its leaves with the xylem water potential of the branch that holds it. g_s was measured with a steady-state porometer LI-1600 (LI-COR Biosciences, USA) in 4–6 leaves per tree.

Twig Huber Value, leaf mass per area and leaf area per twig unit length

The Huber Value (HV) defined as the ratio between sapwood area and leaves area was measured in three terminal twigs per tree. A cross section was made with a scalpel at the base of each twig for the measurement of sapwood and leaf area. Those areas were obtained through high-resolution digital image analysis with the ImageJ software (Schindelin et al. 2015). Subsequently, the leaves were dried in a forced air oven (Venticell, MMM Group, Deutschland) at 70 °C until constant weight for dry matter determination. Leaf mass per area (LMA; g cm^{-2}) was estimated as the ratio between dry mass and foliar area of each sample. Finally, the relationship between leaf area and the length of each twig (uLA; cm^2 cm^{-1}) was calculated.

^{13}C foliar isotopic composition

To measure foliar carbon isotopic composition ($\delta^{13}C$; ‰), a sample of approximately 50 g of fresh mass of fully expanded leaves was taken on the northeast side of each tree considered in the study. The samples were dried in an oven (Venticell, MMM Group) at 70 °C until constant weight and ground using a mortar to form a fine powder to be encapsulated in tin capsules. The isotope composition of two replicates per tree was measured through a standard procedure in the Stable Isotope Laboratory of the Facultad de Ciencias Agronómicas de la Universidad de Chile, with an isotope ratio mass spectrometer (IRMS) model INTEGRA2 (Sercon Ltd Cheshire, UK). The accuracy of the equipment is 0.3 ‰ for $\delta^{13}C$.

Vascular anatomy and theoretical hydraulic conductivity

Anatomical observations were made in the same branches used in WD measurements, on two branch segments per tree. Cross sections of 25-µm thickness were obtained with a sliding microtome REICHERT (Austria). The slices were dehydrated in 50% and 95% alcohol for one and 10 min, respectively. Subsequently, samples were immersed in safranin at 1% aqueous solution for 3 min. Finally, the stained sections were placed in NeoClear® for 10 min and mounted on slides with Canadian balsam.

Sapwood area of the cross sections was photographed in six places selected at random with a digital camera (CANON Esos Revel T5) connected to an optical microscope (Zeiss-Axio Lab.A1, USA) with magnification of 10x, obtaining

photographs of 1.15 mm^2 of sapwood with a resolution of 3.62-pixel μm^{-2}. Images were analyzed with the ImageJ software (Schindelin et al. 2015) using a supervised protocol. The lumen area of each vessel and its number were measured to determine the average vessel area (V_a; μm^2), and vessels density (Vδ; mm^{-2}) as the ratio between the number of vessel in the image and its area (1.15 mm^2). Finally, the average hydraulic vessel diameter (D_{mh}; μm) was estimated as follows (Scholz et al. 2013):

$$D_{mh} = \left(\frac{\sum_{i=1}^{n} D_i^4}{n} \right)^{\frac{1}{4}}, \quad (2)$$

where D is the diameter of the *i*th vessel calculated from its area ($D = \left(4V_a/\pi\right)^{1/2}$), and *n* is the number of vessels considered in the calculation. The fraction of lumen area of vessels (V_f; %) was estimated as the product between V_a and Vδ multiplied by 100 to express it as a percentage, and the vessels composition (S; μm^2) was estimated as the ratio between V_a and number of vessels (Scholz et al. 2013).

The theoretical sapwood-specific hydraulic conductivity (K_{theo}; kg m^{-1} MPa^{-1} s^{-1}) was estimated using the Poiseuille–Hagen law adapted for a set of vessels (Eq. 3; Tyree and Ewers 1991), which indicates that the transport of water through a section of sapwood is directly proportional to the sum of the *i*th diameters of the vessels raised to the fourth power:

$$K_{theo} = \left(\frac{\pi\delta}{128\eta A_s} \right) \sum_{i=1}^{n} \left(D_i^4 \right), \quad (3)$$

where η is the fluid kinematic viscosity (1002×10^{-9} MPa s at 20 °C); δ is the density of the fluid (998.2 kg m^{-3} at 20 °C), D_i is the diameter (μm) of each *i*th xylematic vessel, and A_s is the sapwood area considered in the estimation (μm^2). Finally, a theoretical leaf-specific hydraulic conductivity (K_L; mmol m^{-1} MPa^{-1} s^{-1}) was estimated as the product between K_{theo} and HV (Cruiziat et al. 2002).

Statistical analysis

The variables were compared between descent condition (No_DPL and ++DPL) with a *t* student test. Traits V_a, V_δ, V_f, S, CA and sCSA were transformed with Log_{10}, and ψ_{pd} was raised to the cube, to fulfill the normality assumption. A principal component analysis (represented by a biplot), was carried out as an exploratory analysis of the associations between the variables evaluated in this study (Supplementary Fig. 3). Finally, relationships between traits were analyzed through analysis of covariance defining the condition of DPL as a fixed factor in the regression model.

Results

Hydraulic architecture of *P. tamarugo* and trade-offs observed at whole tree level and branches

Differences were observed in architectural and morphology traits of *P. tamarugo* trees at both whole tree and branch level between conditions of descent of phreatic level (DPL). Trees in No_DPL showed greater height (H), crown area (CA) and total trunk cross-sectional area (sCSA) than ++DPL (Table 1). Arguably, all these trees belonged to the same population and origin before phreatic level descent occurred. No_DPL trees exhibited thinner leaves with a lower leaf mass per area (LMA), and lower Huber Value (HV). HV variation being explained by a greater twig leaf area in No_DPL trees ($P = 0.0047$), with equal sapwood area ($P = 0.582$) between condition of DPL (Table 1).

Descent of phreatic level had no effect on the sCSA ~ H (Fig. 3a) and CA ~ sCSA (Fig. 3c) relationship. Covariance analysis showed a significant effect of DPL only for the CA ~ H relationship, being the intercept significantly greater, and the slope smaller in No_DPL compared to the ++ DPL (Supplementary Table 1). Thus, although there are taller trees in the No_DPL condition, crown area increases at lower rate in No_DPL than ++DPL (Fig. 3b).

Table 1 Comparison of whole tree and branch hydraulic architecture traits of *P. tamarugo* trees between a condition without (No_DPL; $n = 10$) and with severe descent of phreatic level (++DPL; $n = 10$) in the Llamara Salt Flat, Atacama Desert, northern Chile

HA Trait	Significance	No_DPL		++DPL	
		Mean ± S.E.	VC (%)	Mean ± S.E.	VC (%)
H (m)	**	9.4 ± 1.08	36.4	4.4 ± 0.48	34.26
CA (m^2)	***	379.5 ± 64.79	54.0	86.5 ± 25.34	92.6
sCSA (cm^2)	***	3670.1 ± 882.8	76.1	998.7 ± 107.25	34.0
LMA ($g\ cm^{-2} \times 10^{-4}$)	*	140 ± 4.0	8.7	160 ± 7.0	14.2
$HV \times 10^4$	**	8.9 ± 0.95	34.1	13.1 ± 0.82	19.8

H tree height; *CA* crown area; *sCSA* cross-sectional area; *LMA* leaf mass per area; *HV* Huber Value; *VC* coefficient of variation

Significance levels are indicated as $*P < 0.05$; $**P < 0.01$; $***P < 0.001$

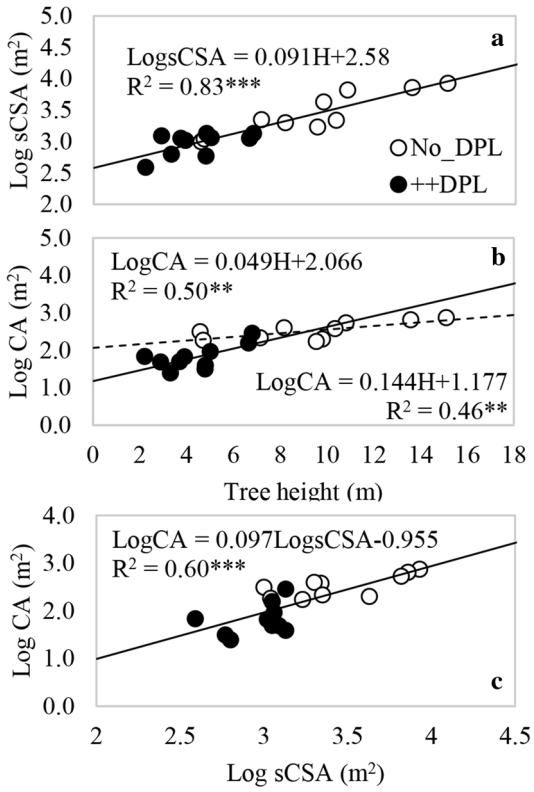

Fig. 3 Relationship between: **a** Total trunk cross-sectional area (sCSA) and Tree height ($n=20$), **b** crown area and Tree height ($n=10$), and **c** crown area and sCSA ($n=20$) of *P. tamarugo* established in a condition without (No_DPL) and with severe descent of phreatic level (++DPL) in the Llamara Salt Flat, Atacama Desert, northern Chile

Performance of *P. tamarugo* in a condition with and without descent of phreatic level

After 12 years, no significant differences were observed between conditions of DPL for g_s (Fig. 4a), $\delta^{13}C$ (Fig. 4b) and Ψ_{pd} (Fig. 4c). However, significant differences were observed for Ψ_{md} (Fig. 4d), having No_DPL trees an average Ψ_{md} of −2.7 MPa, which was significantly higher than ++DPL, with −3.2 MPa. The RER (Fig. 4e) and uLA (Fig. 4f) were significantly greater in the No_DPL than ++DPL.

Comparison of sapwood traits at branch level of *P. tamarugo* between phreatic level conditions

At the branch level (Table 2), ++DPL trees exhibited a greater vessel density (V_δ) and vessels fraction (V_f), and a smaller vessel composition (S) and hydraulic vessel diameter (D_{mh}) than No_DPL. Although mean vessel area (V_a) tended to be greater in No_DPL, the difference was no significant at 5% ($P=0.087$). Something similar happened with the theoretical leaf-specific hydraulic conductivity (K_L), which tended to be higher in ++DPL, although not significant ($P=0.073$). Despite the differences mentioned, no differences in theoretical sapwood-specific hydraulic conductivity (K_{theo}) and wood density (WD) were observed between conditions of DPL.

Intra-specific trade-off between hydraulic efficiency and safety in *P. tamarugo* under descent of phreatic level

V_a was significantly and negatively related to V_δ for both No_DPL and ++DPL (Fig. 5). However, covariance analysis indicated that the slopes of both relations were statistically different ($P=0.0004$), being −0.82 in the No_DPL and −0.41 in ++DPL. The $V_a \sim V\delta$ relationship was much closer to the theoretical specific hydraulic conductivity isoline in the No_DPL condition, whereas in ++DPL the variations observed in V_a were smaller regarding the variation of V_δ.

Covariance analysis indicated that the WD was significantly related to all vascular traits independently of the condition of DPL (Supplementary Table 2), except for K_L and K_{theo} (Fig. 6e, f), where the relationship with WD was non-significant. There were positive relationships of WD with V_a and S (Fig. 6a, d), while V_δ and V_f were negatively related between them (Fig. 6b, c).

Discussion

P. tamarugo adjusts its hydraulic architecture in different levels of integration with homeostatic effects on its performance under descent of phreatic level

Smaller trees in H and CA have been frequently observed under water stress condition. This has been proposed as an adaptive strategies associated with the priority of root growth to avoid water stress (Imada et al. 2008), as well as limiting the length of the hydraulic path and the gravitational hydrostatic gradient (Mennuccini and Magnani 2000; Midgley 2003) posing lower water potentials to distal organs. This might limit processes associated with growth, such as cell elongation and photosynthesis (Ryan et al. 2006). We observed that ψ_{pd}, as a proxy of maximum available soil water content (Richter 1997, Sellin 1999), was similar between conditions of DPL. This could indicate a hydraulic connection between *P. tamarugo* pivotal roots and the water table, allowing a similar water potential equilibrium overnight in tall, leafy trees exposed to ~5 m of phreatic level depth (No_DPL), and short and defoliated trees exposed to ~16 m of phreatic level depth (++DPL). However, ++DPL trees experienced a restriction of its canopy

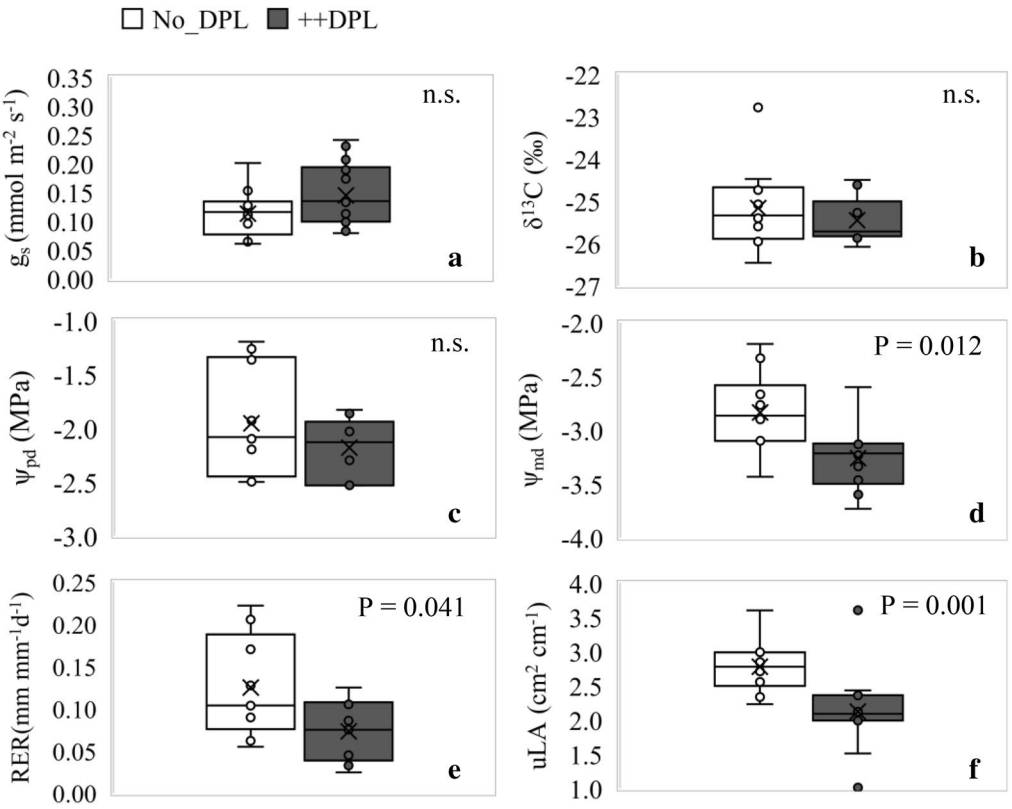

Fig. 4 **a** Stomatal conductance (g_s), **b** foliar ^{13}C isotope composition ($\delta^{13}C$), **c** Predawn water potential (Ψ_{pd}), **d** midday water potential (Ψ_{md}), **e** relative twig elongation rate (RER) and **f** leaf area per unit of twig length (uLA) of *P. tamarugo* established in a condition without (No_DPL; $n = 10$) and with severe descent of phreatic level (++DPL; $n = 10$) in the Llamara Salt Flat, Atacama Desert, northern Chile

Table 2 Comparison of sapwood traits of *P. tamarugo* established in a condition without (No_DPL; $n = 10$) and with severe descent of phreatic level (++DPL; $n = 10$) in the Llamara Salt Flat, Atacama Desert, northern Chile

Traits	Significance	No_DPL		++DPL	
		Mean ± S.E.	VC (%)	Mean ± S.E.	VC (%)
V_a (μm^2)	n.s.	980.2 ± 94.3	30.4	755.5 ± 57.1	23.9
V_δ (mm^{-2})	**	107.7 ± 11.5	33.7	186.2 ± 22.8	38.6
V_f (%)	**	9.2 ± 0.5	18.4	13.1 ± 1.2	28.1
D_{mh} (μm)	*	40.6 ± 1.8	14.3	35.6 ± 1.4	11.9
S (μm^2)	**	10.7 ± 2.1	61.2	4.5 ± 0.8	53.0
K_{theo} (Kg m^{-1} MPa^{-1} s^{-1})	n.s.	6.8 ± 0.6	28.9	7.3 ± 0.8	33.3
WD (g cm^{-3})	n.s.	0.57 ± 0.02	9.8	0.55 ± 0.01	5.9
K_L (mmol m^{-1} MPa^{-1} s^{-1})	n.s.	355.5 ± 65.33	58.1	515.1 ± 52.49	32.23

V_a mean vessel area, V_δ vessel density, V_f vessel fraction, D_{mh} mean hydraulic diameter, S vessel composition, K_{theo} theoretical sapwood-specific hydraulic conductivity, K_L theoretical leaf-specific hydraulic conductivity, *WD* wood density, *VC* coefficient of variation

Significance levels are indicated as: ns $P > 0.05$; *$P < 0.05$; **$P < 0.01$; ***$P < 0.001$

growth, with a lower RER and uLA (Fig. 4), both dependent of turgor pressure, which could indicate that the rate at which water potential balance overnight is different.

During the day, higher HV in twigs which would decrease the dynamic tension of xylem water, increasing the hydraulic capacity per unit of leaf area (Bucci et al. 2008). In fact, no significant difference in K_{theo} and K_L was observed between DPL conditions; however, the trend was at a higher K_L in ++DPL (Table 2). Similar results were reported by Martínez-Vilalta et al. (2009) in Scot pine in an aridity gradient. These adjustments can contribute to maintain hydraulic efficiency under water stress, sustaining the observed similar

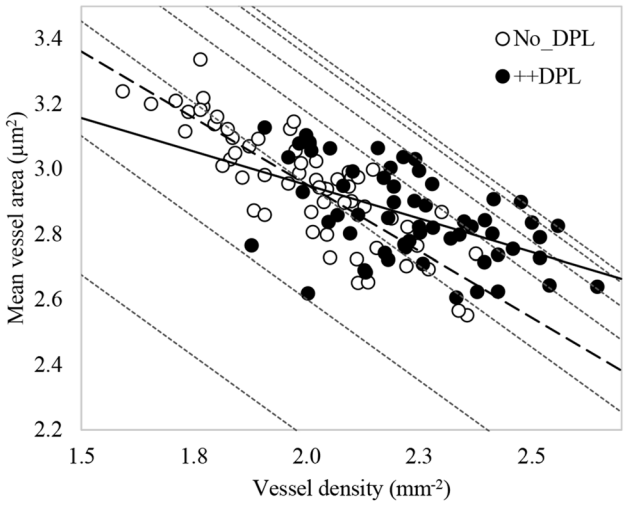

Fig. 5 Relationships between mean vessel area (V_a) and vessel density (V_δ) in log-scaled axes, measured in branches of *P. tamarugo* established in a condition without (No_DPL) and with severe descent of phreatic level (++DPL) in the Llamara Salt Flat, Atacama Desert, northern Chile. Segmented line represents the linear relationship in the No_DPL ($LogV_a = -0.81LogV_\delta + 4.6$; $n = 60$) and solid line represent the linear relationship in ++DPL ($LogV_a = -0.81LogV_\delta + 4.6$; $n = 60$). Thin dotted lines indicate isolines representing combinations of vessel density and size that result in the same theoretical sapwood-specific hydraulic conductivity (Eq. 3)

g_s between DPL conditions (Fig. 4a). Equal $\delta^{13}C$ between conditions of DPL (Fig. 4b) also suggest similar intrinsic water use efficiency (the ratio between assimilation rate and g_s; Farquhar et al. 1982), and therefore a similar assimilation rate per unit of leaf area between DPL conditions.

While theoretical hydraulic efficiency would be high under ++DPL, trees experience lower ψ_{pd} (Fig. 4d). The allometric relationship CA ~ H (Fig. 3) showed that trees in ++DPL tend to have a shrub structure, advantageous in the face of water supply deficit (McDowell and Allen 2015); smaller trees also had open and sparse canopies; therefore, a higher proportion of leaves are exposed to direct radiation and lower aerodynamic resistant due to wind. This is how a greater transpiration rate per unit of leaf area is expected, explaining a lower ψ_{pd} and greater LMA in ++DPL trees, with leaves more tolerant to turgor loss (Bucci et al. 2004) and hydraulic conductance loss (Johnson et al. 2018). Additionally, we observe that taller trees have higher water potentials regardless of the condition of DPL (Supplementary Fig. 2). This is coherent with an allometric equilibrium between above and underground tree biomass (Paul et al. 2019), where bigger trees (like ++DPL trees) could access to more groundwater by deeper roots or less root resistance to water uptake through a greater number of roots.

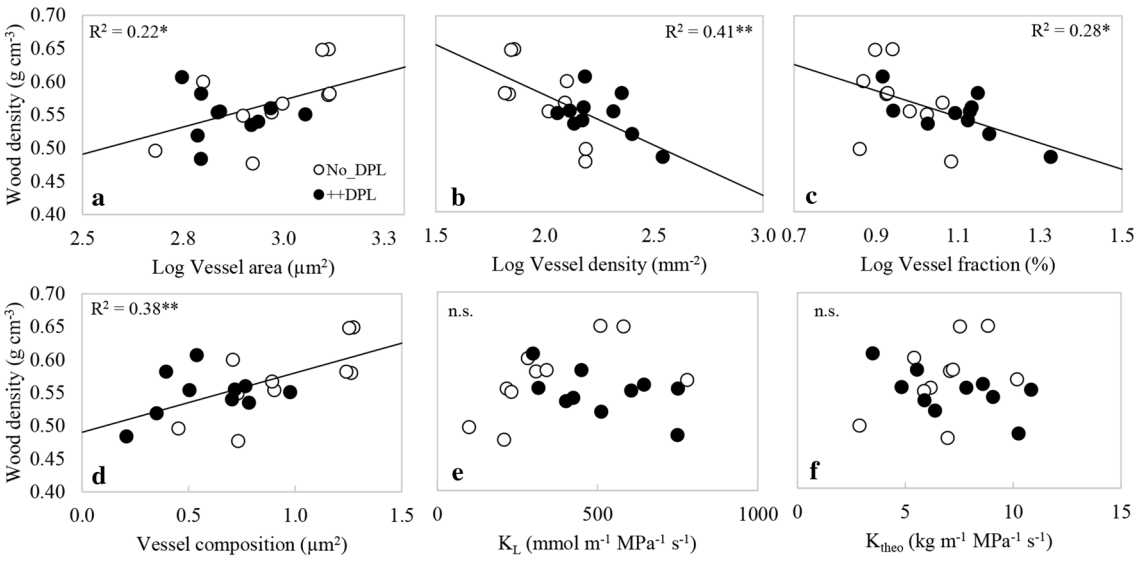

Fig. 6 Relationship between wood density (WD) and the following vascular traits: **a** mean vessel area (V_a), **b** vessel density (V_δ), **c** vessel fraction (V_f), **d** vessel composition (S), **e** theoretical leaf-specific hydraulic conductivity (K_L) and **f** theoretical hydraulic conductivity (K_{theo}) of *P. tamarugo* trees established in a condition without (No_DPL) and with severe descent of phreatic level (++DPL) in the Llamara Salt Flat, Atacama Desert, northern Chile. Significance levels are indicated as: n.s. $P > 0.05$; *$P < 0.05$; **$P < 0.01$; ***$P < 0.001$

The covariation of anatomical xylem traits in *P. tamarugo* under descent of phreatic level compensated maintaining a constant sapwood-specific hydraulic conductivity and wood density

Under both DPL conditions, there was a strong and negative $V_a \sim V_\delta$ relationship (Fig. 5). This has been proposed as a proof of the trade-off between hydraulic efficiency and safety in gymnosperms and angiosperms (Tyree and Ewers 1991; Preston et al. 2006; Poorter et al. 2010), since smaller vessels reduce conductivity and improve cavitation tolerance through a low risk of air-seeding because they have a smaller pit membrane area (Hacke et al. 2006). Although an investment in hydraulic safety in response to a long-term descent of the phreatic level was expected, no difference in V_a and therefore in K_{theo} was observed between conditions of DPL (Table 2). The tendency of smaller mean lumen area in ++DPL (Table 2; Supplementary Fig. 4) was long compensated by a significant increase in V_δ. This explains why a greater vessel composition in No_DPL did not imply a greater K_{theo} as expected (Zanne and Falster 2010; Zanne et al. 2010). In our study, variation in S was mainly due to variation in V_δ, and not to V_a; so no trade-off between safety and efficiency was observed at vascular level.

Unlike what was observed in other studies where the $WD \sim V_a$ relationship was negative (Preston et al. 2006; Hietz et al. 2017), in *P. tamarugo,* this relation was positive. This was to be expected, since by increasing the V_a, V_δ was greatly reduced (V_a and V_f are negatively associated; Supplementary Fig. 2). The above is consistent with a negative relationship between $WD \sim V_\delta$ and $WD \sim V_f$, and a positive relationship between $WD \sim S$ (Fig. 6). However, and despite the observed variability in anatomical traits, e.g. a lower S and greater V_f in ++DPL suggesting an apparent trade-off between hydraulic efficiency and mechanical support (Jacobsen et al. 2005; Zanne et al. 2010; Hietz et al. 2017), WD was not significantly different between conditions of DPL. Similar wood construction cost between conditions of DPL showed that mechanical support in *P. tamarugo* seems to be a priority while deploying vascular adjustments that maintain or maximize water transport efficiency under descent of phreatic level.

Conclusions

After 12 years under descent of phreatic level, *P. tamarugo* deploys a water stress avoidance strategy driven mainly by leaf shedding, sapwood anatomical adjustments, and a possible investment in radical growth in depth. This results in greater twig Huber Values and sapwood vessel density under descent of phreatic level that contributes to improving the theoretical leaf-specific hydraulic conductivity, which tends to be even greater than the control condition, maintaining high stomatal conductance. Although the theoretical hydraulic efficiency is equal between conditions of DPL, *P. tamarugo* trees under descent of phreatic level experience lower water potential possibly due to variables not evaluated in this study, such as the canopy microclimate or root water uptake efficiency.

While the adjustment of aboveground hydraulic architecture traits has a homeostatic effect on *P. tamarugo* performance, it is necessary to advance in the knowledge of the limits of its resistance to descent of phreatic level. In this way, it will be possible to contribute to its conservation in a context of climate change and increasing pressure on its ecosystem due to demographic growth and non-metallic mining, such as the lithium mining in the Atacama Desert.

Author contribution statement MG consived and designed the experiment, collected and analyzed the data, and wrote the manuscript; HB edit and revised the manuscript; JA collected data and revised the manuscript; MO contributed to the measurement of wood anatomical traits and revised the manuscript ; AS contributed to the measurement of ^{13}C isotpe composition and revised the manuscript; EA edit and revised the manuscript. All authors read and approved the final manuscript.

Acknowledgements This study was financed by FONDECYT Project No. 1150799 and the Advanced Human Capital Project CONICYT-PCHA/NationalDoctorate/2015-21150807.

References

Addington RN, Donovan LA, Mitchell RJ, Vose JM, Pecot SD, Jack SB, Hacke UG, Sperry JS, Oren R (2006) Adjustments in hydraulic architecture of *Pinus palustris* maintain similar stomatal conductance in xeric and mesic habitats. Plant Cell Environ 29:535–545. https://doi.org/10.1111/j.1365-3040.2005.01430.x

Aravena R, Acevedo E (1985) The use of environmental isotopes oxigen-18 and deuterium in the study of water relations of *Prosopis tamarugo* Phil. In: Habit M (ed) The current state of knowledge of *Prosopis tamarugo*. Food and Agriculture Organization of The United Nations, NewYork, pp 251–256

Bucci S, Goldstein G, Mainzer F, Scholz F, Franco A (2004) Functional convergence in hydraulic architecture and water relations of tropical savanna trees: from leaf to whole plant. Tree Physiol 24:891–899. https://doi.org/10.1093/treephys/24.8.891

Bucci S, Scholz F, Goldstein G, Meinzer F, Franco A, Zhang Y, Hao G (2008) Water relations and hydraulic architecture in Cerrado trees: adjustment to seasonal changes in water availability and evaporative demand, Brazil. J. Lant Physiol 20:233–245

Calderón G, Garrido M, Acevedo E (2015) *Prosopis tamarugo* Phil.: a native tree from the atacama desert. Ground water table depth thresholds for conservation. Rev Chil Hist Nat 88:18. https://doi.org/10.1186/s40693-015-0048-0

Canham CA, Froend RH, Stock WD (2009) Water stress vulnerability of four *Banksia* species in contrasting ecohydrological habits on the Gnangara Mound, Western Australia. Plant Cell Environ 32:64–72. https://doi.org/10.1111/j.1365-3040.2008.01904.x

Chávez R, Jan G, Clevers W, Herold M, Acevedo E, Ortiz M (2013) Assessing water stress of desert tamarugo trees using insitu data and very high spatial resolution remote sensing. Remote. Sens 5:5064–5088. https://doi.org/10.3390/rs5105064

Cosme L, Schiette J, Costa F, Oliveira R (2017) The importance of hydraulic architecture to the distribution patterns of trees in a central Amazonian forest. New Phytol 215:113–125

Cruiziat P, Cochard H, Améglio T (2002) Hydraulic architecture of trees: main concepts and results. Ann For Sci 59:723–752. https://doi.org/10.1051/forest:2002060

Decuyper M, Chávez R, Copini P, Sass-Klaassen U (2016) A multi-scale approach to access the effect of groundwater extraction on *Prosopis tamarugo* in the Atacama Desert. J Arid Environ 131:25–34. https://doi.org/10.1016/j.jaridenv.2016.03.014

Farquhar GD, O'Leary MH, Berry JA (1982) On the relationship between carbon isotope discrimination and the intercellular carbon dioxide concentration in leaves. Funct Plant Biol 9:121–137

Fortunel C, Ruelle J, Beauchêne J, Fine PVA, Baraloto C (2013) Wood specific gravity and anatomy of branches and roots in 113 Amazonian rainforest tree species across environmental gradients. New Phytol 202:79–94. https://doi.org/10.1111/nph.12632

Garrido M, Silva P, Acevedo E (2016) Water relations and foliar isotopic composition of *Prosopis tamarugo* Phil, an endemic tree of the Atacama Desert growing at three levels of water table depth. Front Plant Sci 7:375. https://doi.org/10.3389/fpls.2016.00375

Garrido M, Silva H, Franck N, Arenas J, Acevedo E (2018) Evaluation of morpho-physiological traits adjustment of *Prosopis tamarugo* under long-term groundwater depletion in the hyper-arid Atacama Desert. Front Plant Sci 9:453. https://doi.org/10.3389/fpls.2018.00453

Hacke UG, Sperry JS, Pockman WT, Davis SD, Mc-Culloh KA (2001) Trends in wood density and structure are linked to prevention of xylem implosion by negative pressure. Oecologia 126:457–461. https://doi.org/10.1007/s004420100628

Hacke UG, Sperry JS, Wheeler JK, Castro L (2006) Scaling of angiosperm xylem structure with safety and efficiency. Tree Physiol 26:689–701

Hietz P, Rosner S, Hietz-Seifert U, Wright SJ (2017) Wood traits related to size and life history of trees in a Panamanian rainforest. New Phytol 213:170–180

Imada S, Yamanaka N, Tamai S (2008) Water table depth affects *Populus alba* fine root growth and whole plant biomass. Funct Ecol 22:1018–1026

Jacobsen AL, Ewers FW, Pratt RB, Paddock WA, Davis SD (2005) Do xylem fibers affect vessel cavitation resistance? Plant Physiol 139:546–556. https://doi.org/10.1104/pp.104.058404

Johnson DM, Berry ZC, Baker KV, Smith DD, McCulloh KA, Domec J-C (2018) Leaf hydraulic parameters are more plastic in species that experience a wider range of leaf water potentials. Funct Ecol 2018(32):894–903. https://doi.org/10.1111/1365-2435.13049

Jupa R, Plavcová L, Gloser V, Jansen D (2016) Linking xylem water storage with anatomical parameters in five temperate tree species. Tree Physiol 36:756–769

Lambers H, Chapin FS III, Pons TL (2008) Plant physiological ecology. Springer, New York

Lehner G, Delatorre J, Lütz C, Cardemil L (2001) Field studies on the photosynthesis of two desert Chilean plants: *Prosopis chilensis* and *Prosopis tamarugo*. J Photochem Photobiol B Biol 64:36–44. https://doi.org/10.1016/S1011-1344(01)00187-7

Leubert F, Pliscoff P (2006) Sinopsis Bioclimática y Vegetacional de Chile. Editorial Universitaria, Santiago de Chile

Maherali H, Pockman WT, Jackson RB (2004) Adaptive variation in the vulnerability of woody plants to xylem cavitation. Ecology 85:2184–2199. https://doi.org/10.1890/02-0538

Martínez-Vilalta J, Cochard H, Mencuccini M, Sterck F, Herrero A, Korhonen JF, Llorens P, Nikinmaa E, Nolè A, Poyatos R, Ripullone F, Sass-Klaassen U, Zweifel R (2009) Hydraulic adjustment of Scots pine across Europe. New Phytol 184:353–364. https://doi.org/10.1111/j.1469-8137.2009.02954.x

McDowell N, Allen C (2015) Darcy's law predicts widespread forest mortality under climate warming. Nat Clim Chang 5:669–672. https://doi.org/10.1038/nclimate2641

Meinzer FC, Johnson DM, Lachenbruch B, McCulloh KA, Woodruff DR (2009) Xylem hydraulic safety margins in woody plants: coordination of stomatal control of xylem tension with hydraulic capacitance. Funct Ecol 23:922–930

Mennuccini M, Magnani F (2000) Comment of "hydraulic limitation of tree height: a critique" by Becker, Meinzer and Wullschleger. Funct Ecol 14:135–140

Midgley JJ (2003) Is bigger better in plants? The hydraulic costs of increasing size in trees. Trends Ecol Evol 18:5–6

Paul K, Larmour J, Specht A et al (2019) Testing the generality of below-ground biomass allometry across plant functional types. For Ecol Manag 432:102–114

Pérez N, Díaz S, Garnies E, Lavorel S et al (2013) New handbook for standardised measurement of plant functional traits worldwide. Aust J Bot 61:167–234. https://doi.org/10.1111/1365-2435.12868

Poorter L, McDonald I, Alarcón A, Fichtler E, Licona J, Peña-Claros M, Sterck F, Villegas Z, Sass-Klaassen U (2010) The importance of wood traits and hydraulic conductance for the performance and life history strategies of 42 rainforest tree species. New Phytol 185:481–492. https://doi.org/10.1111/j.1469-8137.2009.03092.x

Preston KA, Cornwell WK, SeNoye JL (2006) Wood density and vessel traits as distinct correlates of ecological strategy in 51 California coast range angiosperms. New Phytol 170:807–818

Richter H (1997) Water relations of plants in the field: some comments on the measurement of selected parameters. J Exp Bot 48:1–7

Ryan MG, Phillips N, Bond B (2006) The hydraulic limitation hypothesis revisited. Plant Cell Environ 29:367–381

Schindelin J, Rueden CT, Hiner MC et al (2015) The ImageJ ecosystem: an open platform for biomedical image analysis. Mol Reprod Dev 82:518–529. https://doi.org/10.1002/mrd.22489

Scholander PF, Bradstreet ED, Hemmingsen EA, Hammel HT (1965) Sap pressure in vascular plants: negative hydrostatic pressure can be measured in plants. Science 148:339–346. https://doi.org/10.1126/science.148.3668.339

Scholz A, Klepsch M, Karimi Z, Jansen S (2013) How to quantify conduits in wood? Front Plant Sci 4:1–11

Sellin A (1999) Does pre-dawn water potential reflect conditions of equilibrium in plant and soil water status? Acta Oecologica 20:51–59. https://doi.org/10.1016/S1146-609X(99)80015-0

Sperry JS, Saliendra NZ (1994) Intra-and inter-plant variation in xylem cavitation in Betula occidentalis. Plant Cell Environ 17:1233–1241. https://doi.org/10.1111/j.1365-3040.1994.tb02021.x

Sperry JS, Donnelly JR, Tyree MT (1988) A method for measuring hydraulic conductivity and embolism in xylem. Plant Cell Environ 11:35–40

Sperry JS, Mainzer F, McCulloh K (2008) Safety and efficiency conflicts in hydraulic architecture: scaling from tissue to trees. Plant Cell Environ 31:632–645

Sudzuki F (1969) Absorción foliar de humedad atmosferica en tamarugo, *Prosopis tamarugo* Phil. Univ Chil Facult Agron Bol Tecnico 30:1–23

Tyree MT, Ewers F (1991) The hydraulic architecture of trees and other woody plants. New Phytol 119:345–360

Tyree MT, Davis SD, Cochard H (1994) Biophysical perspectives of xylem evolution: is there a tradeoff of hydraulic efficiency for vulnerability dysfunction? IAWA J 15:335–360. https://doi.org/10.1163/22941932-90001369

Zanne AE, Falster DS (2010) Plant functional traits—linkages among stem anatomy, plant performance and life history. New Phytol 185:348–351. https://doi.org/10.1111/j.1469-8137.2009.03135.x

Zanne AE, Westoby M, Falster DS, Ackerly DD, Loarie SR, Arnold SEJ, Coomes DA (2010) Angiosperm wood structure: global patterns in vessel anatomy and its relationship to wood density and potential conductivity. Am J Bot 97:207–215

Zolfaghar S, Villalobos-Vega R, Zeppel M, Eamus D (2015) The hydraulic architecture of Eucalyptus trees growing across a gradient of depth-to-groundwater. Funct Plant Biol 42:888–898

Publisher's Note Springer Nature remains neutral with regard to jurisdictional claims in published maps and institutional affiliations.